Physica B: Condensed Matter

Computational investigation of the effect of ZnS buffer layer on the hole transport of polymer solar cell

--Manuscript Draft--

Manuscript Number:	PHYSB-D-23-00896R2
Article Type:	Research Paper
Section/Category:	Condensed Matter Physics
Keywords:	ZnS nano-particle; Charge transport, Photons-harvesting, Organic solar cell
Abstract:	Semiconductor organic solar absorber exhibits poor charge transport process because of exciton short diffusion length, short life time, and poor carrier mobilities in the medium. Such transport properties have negatively impacted the performance of organic solar cells (OSC). This article is designed to investigate the effect of solar absorber thickness and metal plasmonicnanoparticles using the most popular polymer blend (P3HT:PCBM) via SCAPS device simulation program. Bulk hetero-junction (BHJ) design of OSC has partially addressed the challenges by increasing inter-facial area of the acceptor/donor (A/D) molecules, which boosts the generation of free charges. However, the collection of these charges hindered due to low carrier mobilities in polymer medium. Significant influence of the Zinc Sulfide(ZnS) metal nanoparticles(NPs) have been observed on the performance of OSC at various concentrations. Thus, we are reporting here the effect of absorber layer thickness and ZnSNPs on the charge transport process in OSC.

Reviewer #1: The Reviewer is grateful for the paper revision.
The editorial work significantly improved and clarified the manuscript.
Unfortunately, some of the authors' revisions are irrelevant to the reviewer's comments.

Comment: For example, the authors continue to link changes in the parameters of the solar cell with changes in the values of shunt and series resistances. However, they do not determine the resistance values. Estimating shunt and series resistances from the current-voltage curve is easy!

Reply: Authors have included the series and shunt resistances in the revised manuscript.

Comment: The new figure (Fig.9 in the revised manuscript) has been published previously (Journal of Materials Science: Materials in Electronics, 31, pp 9415-9422, Fig.2b,e). Any mention of previous publications is absent. Moreover, during simulation, the structure depicted in the powder image shown in Fig. 9 is not taken into account, thus making the figure's relevance to this work indirect.

Reply: The reference related to Fig. 9 (now Fig. 8) is cited in the manuscript. We have mentioned [ref. 31] in terms of the effect of ZnS on experimentally fabricated devices. Fig. 9 (now Fig. 8) is used in the manuscript to show the nature ZnS nanoparticles such as size and crystallinity. According to Fig. 8, the size of the nanoparticles are ranges from 4.9 nm to 10 nm as clearly indicated in the TEM image. The particles are formed even less than 5 nm.

Comment: The authors continue to use forward bias instead of reverse bias when constructing the Mott-Schottky. They do not explain why the i) determination of the built-in potential was performed for only one thickness of the absorber layer; ii) a narrow range of the voltage capacitance dependence was chosen.

Reply: Corrected. Initially, authors were able to show the determination of built in potential for one thickness to show example. Now, we have incorporated all thicknesses used in the investigations. The reason behind narrow range voltage chosen is because of the low operating voltage of organic solar cell.

Comment: The new highlight ("Polymer solar absorber thickness has significant impact on the performance the solar cell") is far from the original result.

Reply: The authors have changed the highlight to the main focus the manuscript. “The thickness of ZnS layer in the device architecture makes significant impact on the performance the solar cell”

Comment: The authors stated "The scale of Fig. 4 is improved in the revised manuscript." In fact, Fig. 4 remained unchanged in the revised manuscript.

Reply: The main problem with the scale was the low values of the Voc compared to other

parameters, which is less than 1. We plotted Voc separately from the rest in the revised manuscript.

Comment: The authors stated "The data in Table II and Table III are not the same.". But comment stated that the data in Table II duplicate Figure 4. In the revised manuscript, data duplication remains.

Reply: The data in the two tables are not representing the parameters of the solar cells of the same kind. The values might look similar but are not drawn from the same samples. Table II consists of values from those devices without ZnS and Table III contains results of solar cells from ZnS included devices. The captions of the tables are revised.

Comment: A few new inaccuracies have appeared in the revised manuscript. For example, the new abbreviation TFOSC is not deciphered. Works [32] and [31] have nothing to do with the equations (12) and (14).

Reply: The citation of the references are corrected in the revised manuscript.

If the authors of the paper so desire, all of the aforementioned shortcomings can be rectified. However, there are two reasons why I cannot recommend accepting the paper:

Comment: 1. The paper does not model any plasmonic effects, meaning the title of the manuscript does not match its content.

Reply: The authors have modified the title according to the referee's suggestions. Now the title reads "Computational investigation of the effect ZnS buffer layer on the hole transport of polymer solar cell".

Comment: 2. Using a ZnS layer with a thickness of 3 nm does not result in the formation of nanoparticles in 1D simulation. Therefore, the active use of the term "metal nanoparticles" in the paper, conclusions, and highlights is unfounded.

Reply: Authors are grateful for this referee comment. According to Fig. 8, the size of the nanoparticles ranges from 4.9 nm to 10 nm as clearly indicated in the TEM image. The authors do believe that the particle can form around 5 nm range, as we closely check the images the particle size might go down to 4.5 nm. We have modified the thickness of ZnS from 5 nm to 11 nm in the revised manuscript. Additional comments are also given in relation to this thickness.

Reviewer #3: I am satisfied with the changes made to the manuscript and I recommend publication.

Computational investigation of the effect ZnS buffer layer on the hole transport of polymer solar cell

Ncedo Jili[1], Nkosinathi Dlamini[1], Genene Tessema Mola[1*]
[1] *School of Chemistry & Physics, University of KwaZulu-Natal, Pietermaritzburg Campus,Private Bag X01, Scottsville 3209, South Africa*
(Dated: June 21, 2023)

Semiconductor organic solar absorber exhibits poor charge transport process because of exciton short diffusion length, short life time, and poor carrier mobilities in the medium. Such transport properties have negatively impacted the performance of organic solar cells (OSC). This article is designed to investigate the effect of solar absorber thickness and metal plasmonic nanoparticles using the most popular polymer blend (P3HT:PCBM) via SCAPS device simulation program. Bulk hetero-junction (BHJ) design of OSC has partially addressed the challenges by increasing inter-facial area of the acceptor/donor (A/D) molecules, which boosts the generation of free charges. However, the collection of these charges hindered due to low carrier mobilities in polymer medium. Significant influence of the Zinc Sulfide(ZnS) metal nanoparticles(NPs) have been observed on the performance of OSC at various concentrations. Thus, we are reporting here the effect of absorber layer thickness and ZnS NPs on the charge transport process in OSC.

PACS numbers: 73.61.ph; 73.61 Wp

Keywords: ZnS nano-particle; Charge transport, Photons-harvesting, Organic solar cell

I. INTRODUCTION

Semiconductor polymers have attracted numerous research interests because of its application in photonic devices such organic solar cells (OSCs), organic light emitting diode(OLD), organic sensors etc. The market values organic molecules-based device is continuously growing by the introduction of new technology and applications. This article is trying to discuss some of the challenges of thin film organic solar cell. Organic solar has been under intense investigations for the past three decades due to its potential to generate cheap renewable energy from low cost solar panel. OSC is one of the few emerging solar cell technologies which is evolving to have high power conversion efficiency (PCE) required for mass production [1]. Hence, OSCs are expected to contribute towards renewable energy sector with high potential of reducing cost of device production, light weight, and flexible solar panel [2]. Even though OSCs offer such attractive features but they have drawback in terms of short life time, low efficiency and prone to oxygen and humidity that limits its penetration into energy market [3]. The first Photo-voltaic solar cell was fabricated from crystalline silicon in 1950s at the Bell laboratory. Since then the PCE of silicon based solar cell increases and approaching currently the theoretical limit 30% [4]. On the other hand, organic solar cells were introduced around 1990 [5] and the PCE continuously increasing to nearly 20% from single junction non-fullerene based OSC. The efficiency of OSCs remains low relative to other emerging and established solar cell technologies due to the poor charge transport processes in organic medium.

Bulk heterojunction is the most successful design of solar absorber in OSC which creates large donor/accepter molecules interfaces for enhanced exciton dissociation [6]. Furthermore, BHJ is allowing an efficient charge dissociation by reducing recombination processes in the photo-active medium. Consequently, the OSCs research gained significant attention because of continuous growth in PCE. However, fullerene based OSC has an efficiency close to 14% because of poor energy band tunability and narrow optical absorption [7–10]. One of the challenges in polymer solar cell is the short diffusion length of the excitons, which limits the thickness of the absorber layer to $\leq$200 nm for sufficient charge generation. In this report, we have investigated the effect of ZnS doped hole transport layer and thickness dependence absorber layer on the performance of thin film solar cells. We employed device simulation program known as solar cell capacitance simulator (SCAPS) which is a one-dimensional device simulation program to investigate the effect of changes on the parameters under investigation. The metal nanoparticles in dielectrics medium exhibits a phenomenon called Local Surface Plasmon Resonance (LSPR) due to the interaction with incident electromagnetic radiation. The excitation of LSPR de-phases through a number of channels including, generation of hot electrons, near field enhancement, charge transfer, energy transfer and light trapping through scattering [11–13]. This investigation takes into account of the advantages of metal nanoparticles on improving charge dissociation and light trapping processes in the functional layers of the solar cell. The article is composed of background theory of metal plasmon, device simulation and discussion of the results.

*E-mail me at: mola@ukzn.ac.za

II. LOCALIZED SURFACE PLASMON RESONANCE

The interaction between the incident electromagnetic (EM) radiation and metal nanoparticle in dielectric medium leads to the polarization of the surface charge on the metal nano-particles resulting in the excitation of surface charge plasmon resonances. Figure 1a depicts the electric field component of EM field displaced the surface electron plasma of the metal to one direction creating a dipole moment that oscillate at the frequency of the incident radiation. This oscillation stores energy that dephase in the form generating hot electron or other forms energy transfer. The occurrence of LSPR is dependent on the size, shape, position, and the geometry of nanomaterial [14–17].

The generation of hot electrons exhibited in the form optical absorption whose absorbance can be expressed according to eq(1) derived from Mie theory of classical electromagnetic light scattering. The absorption and scattering cross section are given by [14].

$$C_{abs} = \frac{2\pi}{\lambda} Im[\alpha] \,, \tag{1}$$

and,

$$C_{scatt} = \frac{1}{6\pi}\left(\frac{2\pi}{\lambda}\right)^4 |\alpha|^2 \,. \tag{2}$$

where λ is the electromagnetic field wavelength, and α is the polarizability of the particle which is given by

$$\alpha = 3V\frac{\omega_p^2}{\omega_p^2 - 3\omega - i\gamma\omega} = 3V\left[\frac{\varepsilon_p/\varepsilon_m - 1}{\varepsilon_p/\varepsilon_m + 2}\right] \,, \tag{3}$$

where V is the particle volume, ε_p is the dielectric function of the particle and ε_m is the dielectric function of the embedding medium.

The excited electrons are sometimes referred as the hot-electrons. These generated hot-electrons will be available for photo-generated current in semi-conductors Figure 1b. Another forms of de-phasing the LSPR excitation is the formation near field which scattered light from the nano-particles into the medium [17–19]. The scattering of light in the semi-conductor medium increases optical pathlength of the light. This is a processes in which light scatters multiple times within or near the semi-conductor such that the light remain longer in the semi-conductor medium until it is efficiently absorbed by the material.

III. DEVICE ARCHITECTURE AND NUMERICAL SIMULATION

Organic solar cell is composed of layers of different materials for different roles in the function of the solar cell. The schematic representation of the solar cell structure provided in Figure 2 consists of layers of materials with different thickness. This architecture known as conventional device structure is commonly used in the preparation of thin film organic solar cell experimentally. Solution processed thin film organic solar cell is fabricated on Indium Tin Oxide(ITO) coated glass substrate followed by a hole transport layer (HTL), photo-active layer, electron transport layer(ETL) and a Cathode. The photo-active layer used in this investigation is composed of poly(3-hexylthiophene) and [6,6]-phenyl C61-butyric acid methylester (PCBM) blend (P3HT:PCBM). Whereas the charge transport layers are poly(3,4-ethylenedioxythiophene) polystyrene sulfonate (PEDOT:PSS) (HTL), Lithium Fluoride(LiF)(ETL), Aluminium (Al) as a cathode. The structure remains unchanged for the study of the impact of ZnS in solar cell performances except the insertion of thin ZnS buffer layer. The same device structure is used in all SCAPS simulations.

The device simulation program SCAPS is a one dimensional simulation programme developed at the department of Electronics and Information Systems (ELIS) of the University of Gent, Belgium by a group of researchers listed in references [20–24]. The SCAPS simulator numerically solves the set of one-dimensional transport equations, by firstly discretizing them and uses the Gummel iteration method and Newtons Raphson to solve these equations. Within the bulk of the layers these equations are given by [20, 21].

$$\frac{\partial}{\partial x}(\varepsilon\frac{\partial\psi}{\partial x}) = -\frac{q}{\varepsilon_0}\left[-n + p - N_A^- + N_D^+ + \frac{\rho_{def(n,p)}}{q}\right] \,, \tag{4}$$

$$-\frac{\partial J_n}{\partial x} + G - U_n = \frac{\partial n}{\partial t} \,, \tag{5}$$

$$-\frac{\partial J_p}{\partial x} + G - U_p = \frac{\partial p}{\partial t} \,. \tag{6}$$

Along with the following constitutive equations

$$J_n = -\frac{\mu_n n}{q}\frac{\partial E_{F_n}}{\partial x} \tag{7}$$

$$J_p = -\frac{\mu_p P}{q}\frac{\partial E_{F_p}}{\partial x} \,. \tag{8}$$

In this set of equations n and p have been used to denote the free carrier concentrations. $-N_A^-$ and N_D^+ represent the charged dopant's concentrations. ρ_{def} is the defect distribution. The electron and hole current densities and denoted by J_n and J_p respectively. The net recombination rates given by U_n and U_p, while the generation rate is given by G. The generation rate may be calculated using the following set of equations [7, 8, 18]

$$G(x,\lambda) = \frac{1}{2}c\epsilon\alpha n|E(x)|^2 \tag{9}$$

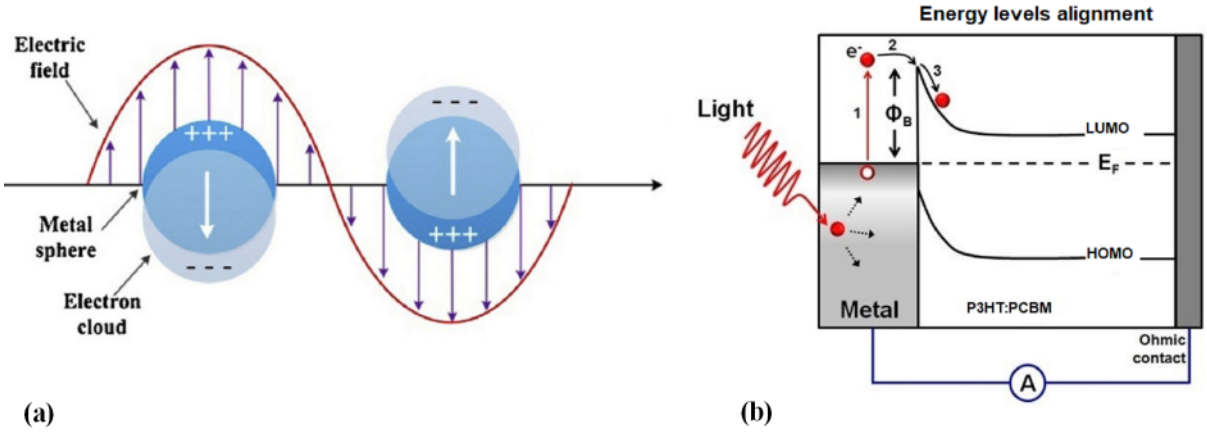

FIG. 1: a) The schematic diagram of LSPR [29], b) Schematic representation of the energy levels alignment and photogenerated electrons injection at metal/semiconductor interface [18]

TABLE I: P3HT:PCBM and ZnS NPs simulation parameters

Parameter	symbol	ITO	PEDO:PSS	P3HT:PCBM	ZnS Nps	units
Thickness	d	80	60	variable	variable	nm
Energy band gap	E_g	3.6	2.2	1.8	3.5	eV
Electron affinity	χ	4.8	4.4	3.8	3.8	eV
Di-electric permittivity(relative)	ϵ	8.9	10	3.8	10	
CB effective density of states	N_C	1.1×10^{19}	1×10^{19}	1×10^{19}	1×10^{20}	cm^{-3}
VB effective density of states	N_V	1.1×10^{19}	1×10^{19}	1×10^{18}	1×10^{19}	cm^{-3}
electron thermal velocity	v	1×10^{7}	1×10^{7}	1×10^{7}	1×10^{7}	$cm\,s^{-1}$
hole thermal velocity	v	1×10^{7}	1×10^{7}	1×10^{7}	1×10^{7}	$cm\,s^{-1}$
electron mobility	μ_n	10	0.001	0.01	160	cm^2/Vs
hole mobility	μ_p	10	0.0001	0.001	5	cm^2/Vs
doping concentration of acceptors	N_A	1×10^{12}	1×10^{14}	0	1×10^{16}	cm^{-3}
doping concentration of Donors	N_D	1×10^{17}	1×10^{15}	0	1×10^{17}	cm^{-3}

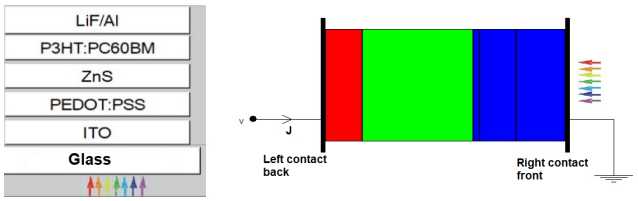

FIG. 2: The conventional solar cell structure in SCAPS

$$G(x,\lambda) = \frac{\lambda Q(z,\lambda)}{hc} \tag{10}$$

$$G(\lambda) = \int_{1.5G} Q(x,\lambda)d\lambda \tag{11}$$

where c is the speed of light, α is the absorption coefficient, and Q represents the energy dissipation. The physical parameters of the materials given in Table 1 are taken from literatures [22–28, 39].

IV. DEVICE SIMULATION RESULTS

A. The effect of absorber layer thickness

Photo-generated exciton has short diffusion length in polymers blend solar absorber medium, and consequently, the absorber layer thickness plays a critical in the performance of OSC. A number of device simulations were conducted in this investigation using P3HT:PCBM solar absorber layer of the solar cell. The absorbers thickness were varied from 120 nm to 300 nm to study the device performances. The simulations were carried out under a 1 Sun illumination ($1000\,W\,m^{-2}$) A.M.1.5G and with the necessary physical parameters of the different functional layers of the solar cell (Table 1). Consequently, Figure 3 represents the simulations results of the J-V curves for active layer thickness's ranging from 120 nm to 300 nm. The main solar cell parameters found from the device simulation are provided in Table 2. These device parameters agree with the experimental results found in reference [30, 31]. According to the results given

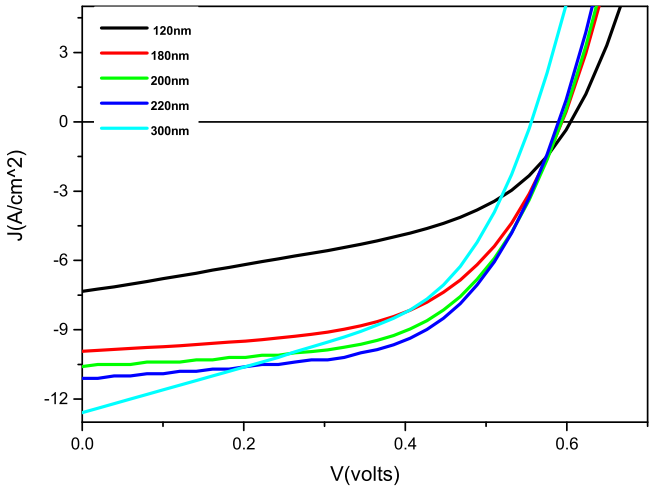

FIG. 3: The J-V curves of P3HT:PCBM at different absorber layer thickness

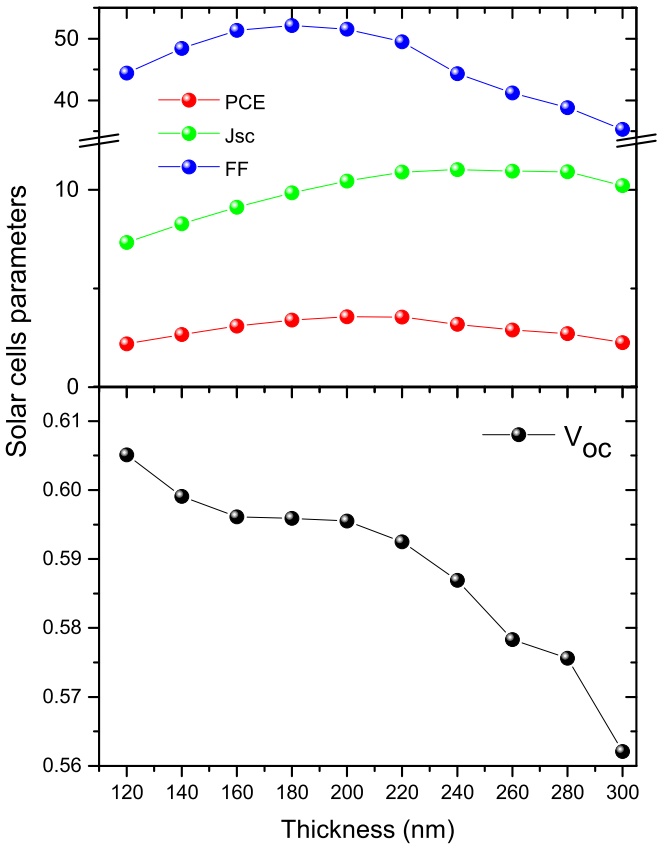

FIG. 4: The solar cell parameters derived from device simulation plotted against absorber layer thickness

in Figure 3, the photo-current found from the device with absorber thickness 120nm was lower than the other devices. It is in fact generated the least power conversion efficiency (see Table 2), which is attributed to low optical absorption and significant amount of incident light escaped unnoticed by semitransparent absorber film. But, as the thickness increases the power conversion efficiency also increases because of the enhanced photo-current and more photons absorptions. The maximum power conversion efficiency found in the simulation was at an absorber layer thickness 200nm. This variations of absorber layer thickness in the devices basically affected almost all device parameters such as Jsc, FF and PCE. The highest performance of P3HT:PCBM based solar cell is observed at the thickness ranging from 180 nm to 220 nm, which is consistent with best OSC fabricated in the laboratory using same polymer blend. The variations in device parameters with thickness of the active layer are given in Figure 4. The FF rose from the minimum 48 % at 120 nm to 52 % at the thickness of 220 nm. The short current density increases from 7.336 mA cm^{-2} at the thickness of 120 nm to 10.89 mA cm^{-2} at the thickness of 220 nm. This improvement is due to the increased photons absorption which resulted in enhanced photo-generated current.

According to the results provided in Figure 4 the V_{oc} slightly varied from 0.5615 V -0.6052 V for both simulated and experimental results [32]. This is due to the fact that the V_{oc} is mostly dominated by the difference in energy levels of lowest unoccupied molecular orbital (LUMO) of the acceptor material and the highest occupied molecular orbital(HOMO) of the donor material [32] as well as the work function of the electrode. However, significant growth in V_{oc} is recorded at thickness $>$ 220 nm, which has contributed to best power conversion efficiency 3.57 %. All the device parameters are decreasing as the thickness increases beyond 220 nm, including the V_{oc} , FF, and J_{sc}, confirmed by device simulation results (Table 2). The V_{oc} decreases from 0.5925 V to 0.562 27 V, and similarly, the Fill Factor drops from 52 % to 35 %, which is attributed to the changes in series resistance and shunt resistance of the devices. The shunt resistance prevent the leakage through the current pathways. The shunt resistance decreases with increasing thickness while the series resistance increases with thickness [29] because the polymer medium become more resistance to current flow as polymer medium get thicker. Furthermore, the life time of photo-generated excitons is low because of it's short diffusion length in polymer medium, and hence, optimum layer thickness is necessary to balance sufficent optical absorption and exciton life time. Therefore, increasing absorber thickness means high the series resistance which reduces the value of the FF. The short current density is also affected by generation, recom-

bination rate and built in electric field [32]. As it can be seen from Poisson's continuity equations eq(7) and eq(8), the solution of the current J(v) explicitly depends on the recombination and generation coefficients. Large thickness results in the high recombination [29–32] of carriers thus carriers lose energy in the form of heat. Increasing thickness decreases the built in electric field, which therefore leads to an excitton dissociation failure, since the exciton is separated by the electric field at donor-acceptor interface[31, 32]. The quantum efficiency of the simulated solar cells, which is defined by the ratio of the number of collected charge carriers divide by the number of incident photons is given in Figure 5. The EQE is calculated for different thickness of the active layers (120 nm, 220 nm, 300 nm), which has significant conversion yield from 350 nm to 650 nm wavelengths of the incident photons. This is mainly determined by the absorbency of the P3HT:PCBM blend. Thus, the EQE yield is dependent on the absorber thickness which shows maximum yield at 300 nm (blue) and followed by minimum at 120 nm layer thickness. The maximum

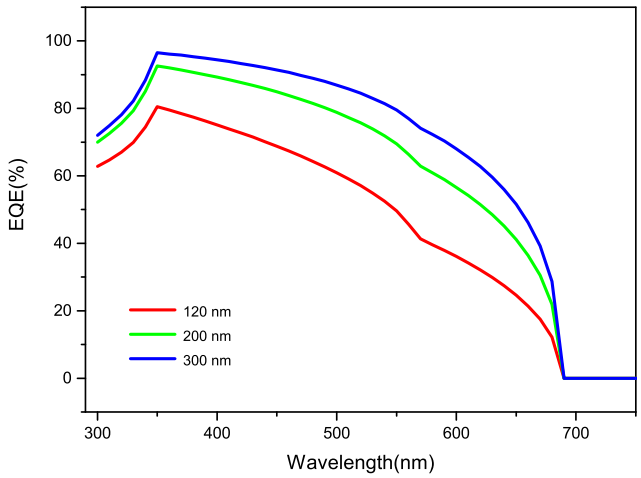

FIG. 5: The External Quantum Efficiency plotted against the incident light wavelengths

EQE peak recorded in the simulations was found to be at 360 nm incident wavelength, where 80 %, 90 % and 95 % are measured at 120 nm,220 nm, and 300 nm, respectively.

B. Capacitance Voltage plot of the devices

The interfaces between the active layer and electrodes is the region of interest when looking at the built in potentials as well as capacitance generated due to the accumulation of charges at the interface [34, 36]. Indeed, OSC has very thin inter-facail buffer layers which can diffuse into active layer in the process of device fabrications. The accumulation of space charge at the interfaces produces capacitance at the metal/semiconductor contact, which is an important parameter to understand the inter-facial conditions in solar cells (Fig. 1b). The information extracted from capacitance in response to applied voltage or frequency is affected by built-in potential and doping density (in C-V plots). The capacitance is defined by equ (12) [35]

TABLE II: Device parameters of P3HT:PCBM based solar cell at various active layer thickness

Thickness (nm)	V_{oc} volts	J_{sc} mA/cm^2	FF %	η %	R_s Ω cm^2	R_{sh} Ω cm^2
120	0.6051	7.33	44.4	2.19	2.8	170
180	0.5959	9.84	52.1	3.40	6.3	940
200	0.5955	10.43	51.5	3.57	8.1	740
220	0.5925	10.89	49.5	3.55	9.9	440
300	0.5621	10.21	35.3	2.25	24.5	100

$$C = \frac{\varepsilon_0 \varepsilon_r A}{w} \tag{12}$$

where ε_0 and ε_r are the permittivity of free space and dielectric medium. whereas A is inter-facial area while w is the width of depletion region, which can be expressed by an equation of the form :.

$$w = \sqrt{\frac{2\varepsilon_0 \varepsilon_r (V_{bi} - V)}{qN}} \tag{13}$$

where V_{bi} is built in voltage, V is bias voltage, q is the elementary charge, and N is the doping concentration given by equ (14) [36].

$$N = \frac{N_A N_D}{N_A + N_D} \tag{14}$$

where N_A and N_D being the doping concentration of acceptor and donor impurities, respectively.

According to the calculated device capacitances presented in Figure 6, the capacitance is decreasing in a reverse bias condition, where depletion layer is large, while it is increasing in forward bias voltages of the solar cell [35]. This is expected from the fact that more charges are crossing the interface in the forward bias, because smaller depletion width, than the reverse bias condition. Furthermore, the capacitance of the devices decreases with thickness of the absorber layer, which is an indicative of the low concentrations of charges at the interfaces in thick polymer active layers. In other words, as thickness of the active layer gets larger, it increases the width of the depletion region, which results in charge recombination hence the capacitance gets reduced in thick layers

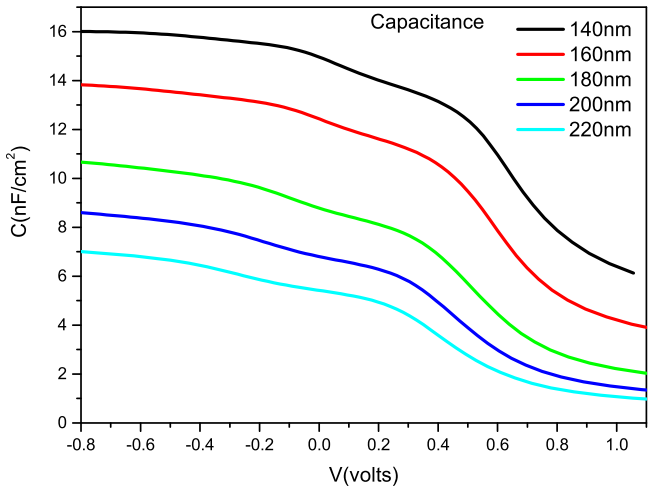

FIG. 6: The capacitance voltage plot of the Pristine with various absorber thickness

(see equ(12)). Similarly, there is a possibility of either the photon-generated charges are collected by the electrodes or neutralised by recombination processes. This agree with the fact that optimized thick active layers are performing better in terms of producing high power conversion efficiency.

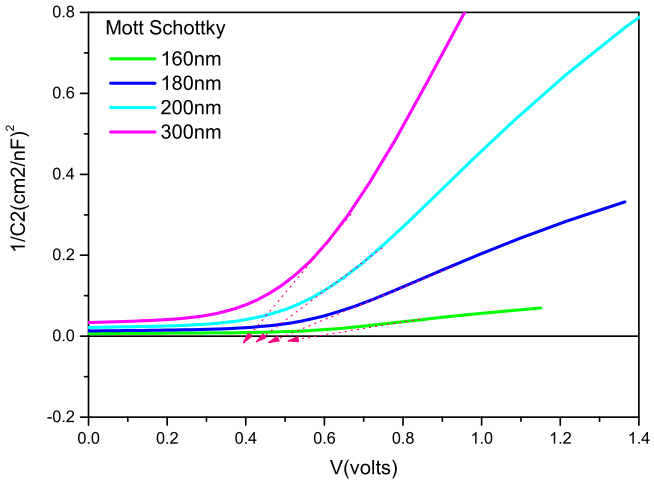

FIG. 7: The Mott Schottky plot of the P3HT:PCBM based active layer with the thickness varied from 160 nm to 220 nm

In an effort to determine the built in potential from the simulation data, Mott Schottky plots are drawn as provided in Figure 7. The plots are defined by the inverse square of the capacitance equation, which is often refereed as the Mott Schottky equation and expressed by equ (15) [37]. **The built in potential can be determined by extrapolation using a straight line tangent to the curves that cross the horizontal axis (see Figure 7). Hence, the x-intercepts of the straight lines are found to be V_{bi} = 0.57 volts, 0.51 volts, 0.46 volts and 0.41 volts, respectively for thickness 160 nm, 180 nm, 200 nm and 300nm.** These values are a reasonable estimate of the built in potentials, which are comparable to the open circuit voltage of P3HT:PCBM based solar cells.

$$C^{-2} = \frac{2(V_{bi} - V)}{\varepsilon_0 \varepsilon_r A^2 q N} \tag{15}$$

Furthermore, the inverse square of the capacitance gives a linear relationship with the voltage. It's slope is used to find the doping concentration while the x-intercept is used to determine the built in voltage [36]. In some literatures, it is reported about the inadequacy of Mott Schottky plot to determine the built in potential and the doping density. However, the result found in the current calculations is not far from the expected.

C. The impact of ZnS NPs on device performance

The effect of ZnS on the performance of thin film polymer solar cell is invetigated using device simulation program. At the moment, the SCAPS program, which uses transport equations for device simulation, is not able to include LSPR effect into fundametal equations. However, the approach used in this investigation is to introduce a very thin layer of ZnS between the photo-active layer and hole transport layer as depicted in Figure 2 to study its impact on device performance. All the functional layers of the device structure are kept at a constant thickness including absorber layer thickness chosen to be 180 nm. However, the ZnS layer thickness is allowed to vary with view to change the concentrations of NPs in the device structure. The ZnS NPs were chosen because of their broad application areas such as blue lighting emitting diodes, solar cells and field emission devices [38]. **Our group have succesfully used ZnS, as dopant in absorber layer of P3HT:PCBM blend, which has produced an improved performance [31]. Dlamini et al. observed enhanced optical absorption from ZnS due to electron band to band transition, which is evident on absorption at low wavelength region [31]. Moreover, ZnS induces light scattering at the interface which increase optical path length in polymer medium that eventually assist light trapping.** Furthermore, by improving conductivity between interfaces ZnS enhances collection of charges. The morphology of ZnS powder, as presented in Figure 8, is taken using high resolution tunnelling electron microscopy (TEM). **The TEM image shows a highly crustalline microstructures with crystal spacing 0.31 nm, and a particle size ranging from 4.9 nm to 10 nm, which an important property for**

charge transport across the layers. Several studies suggest that metallic NPs play important roles at different functional layers of OSC [11–13]. In this work, ZnS

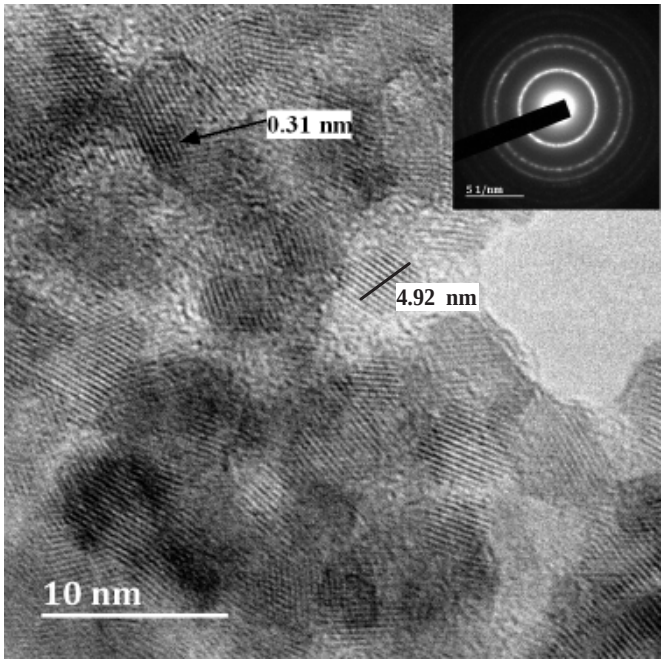

FIG. 8: The TEM image of ZnS powder clearly showing size and crystalline nature of the material.

layer thickness was varied from 5 nm to 11 nm, and consequently, several calculation was conducted to determine performance of the devices. The J-V curves provided in Figure 9 shows the impact of ZnS thickness on the device performances. The best power conversion efficiency recorded in this study was 4.07 %, with parameters as FF = 61.17 %, Jsc = 10.26 mA cm^{-2}, and the Voc = 0.5835 V (as shown in Figure 9 and Table 3). This performance is better than those devices without ZnS layer, and hence, the PCE grew by 19% from the reference cell. Generally, all the device parameters are enhanced by the incorporation of ZnS NPs in the device structure compared to devices without ZnS. The optimum thickness of the ZnS layer for efficient device performance is 5 nm, which exceeds almost in all device parameters (see Table 3). According to the observed results, increasing the ZnS NPs thickness(beyond 6nm) is unfavourable for device performances. Especially, when the band gap of the ZnS layer is beyond 2.5 eV. It has been observed in many experiments [1–3], that the large concentration of NPs in absorber layers result in poor performing devices [11, 12]. This is attributed to the generates unwanted defects concentration at high doping level of nano-particles in a device that can promote charge recombination and leading to poor device performance. Furthermore, high concentration of NPs increases the series resistance and lowers the shunt resistance, which limits the maximum power that can be drawn from the device.

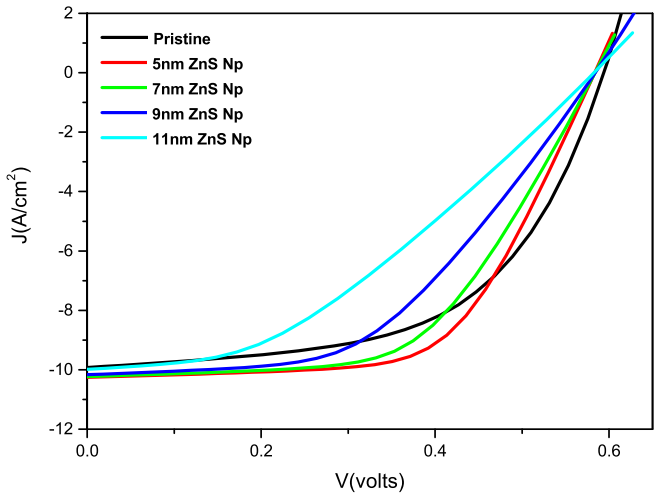

FIG. 9: The J-V curves of P3HT:PCBM + ZnS Nps at different thickness of ZnS Nps

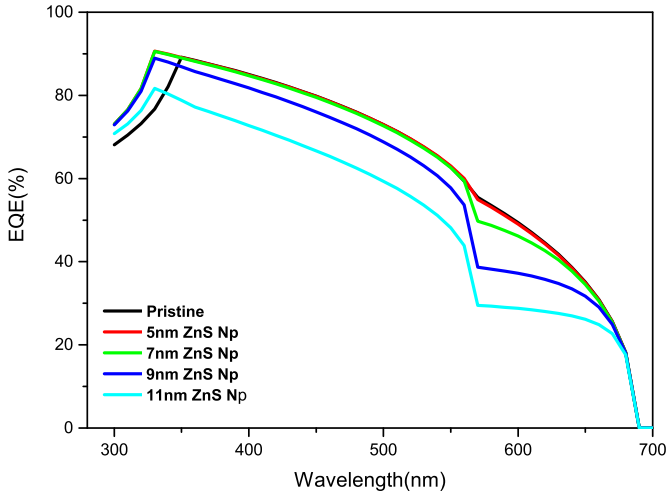

FIG. 10: The External Quantum efficiency plotted against the ZnS Np thickness

The quantum efficiency of the solar cells with ZnS is calculated using various thickness of ZnS layers (Figure 10), which shows a distinct changes in the values of the calculated EQE with the thickness of ZnS. The EQE drops drastically as the ZnS thickness is increased from 7 nm to 11 nm, which signifies the occurrence of charge recombinations in the photoactive medium. Even the high energetic photons are less absorbed when the the ZnS NPs has the thickness of 11 nm. Similarly, the EQE drops to below 82 % as the thickness is increased from 9 nm to 11 nm.

TABLE III: Solar cell parameters of P3HT:PCBM/ZnS absorber at different ZnS thickness

ZnS thickness (nm)	V_{oc} volts	J_{sc} mA/cm^2	FF %	η %	R_s $\Omega\,cm^2$	R_{sh} $\Omega\,cm^2$
0	0.5959	9.8484	52.13	3,40	6.3	940
5	0.5835	10.26	61.2	4.07	3.10	1960
7	0.5840	10.23	56.7	3.77	5.1	1700
9	0.5841	10.17	49.0	3.23	10.2	1450
11	0.5828	9.98	37.9	2.45	19.8	1000

V. CONCLUSION

With the aid of device simulation programme, appreciable solar cell parameters were recorded from the study of absorber layer thickness dependence and the effect of ZnS layer on the performance of OSC. In the first part, the thickness of the photo-active layer (P3HT:PCBM blend) was varied from 120 nm to 300 nm, in device simulation, to see the role of thickness on device performance. The results clearly suggested that absorber thickness indeed affected device performance because of the short diffusion length of the exciton in polymer medium. However, lowering the thickness too much is not favourable either, and thus, the optimum absorber thickness found in the study were from 180 nm to 220 nm. The highest efficiency achieved in P3HT:PCBM blend absorber was 3.57 % at 200 nm thick absorber layer, which agrees with the experimental results. As the thickness of P3HT:PCBM exceeds beyond the optimum range all the device parameters dropped and device performances gets lower. Therefore, the thickness of active layer plays an important role in designing OSC devices. Another independent investigations conducted, by employing ZnS nano-particles in the device structure, with the view to increase performance and charge transport processes. This study has demonstrated that ZnS layer is indeed influenced the device performance of P3HT:PCBM based solar cell. However, the high concentration of ZnS in the device structure negatively impacted the solar cell parameters. Therefore, the maximum efficiency recorded in this study was 4.07 % at the thickness of 5 nm ZnS NPs, which is 19% growth in PCE from solar cells without ZnS. These results suggest that ZnS NPs can be used as a mechanism to trap light in polymer medium and improve the conductivity between the PEDOT:PSS and P3HT:PCBM interfaces. It can also be used as acceptor material due to it's high electron affinity, which can assists in exciton dissociation in polymer.

Declaration of competing interest

The authors declare that they have not known any competing financial interests or personal relationships that could have influenced the work reported in this paper.

Acknowledgments

This work is supported by the National Research Foundation (NRF) (Grant Nos., 85589, 113831), South Africa. The authors also appreciate the Microscopy and Microanalysis Unit (MMU) staff at UKZN for several SEM and TEM measurements.

[1] Abdulrazzaq, O.A., Saini, V., Bourdo, S., Dervishi, E. and Biris, A.S.,2013. Organic solar cells: a review of materials, limitations, andpossibilities for improvement. Particulate science and technology, 31(5), pp.427-442.

[2] Samanta, M., Chattopadhyay, K.K. and Bose, C., 2018, November. A Simulation Based Comparative Study of P3HT: PCBM and OC 1 C 10 PPV: PCBM Organic Solar Cells. In 2018 IEEE Electron Devices Kolkata Conference (EDKCON) (pp. 218-221). IEEE.

[3] Clare Dyer-Smith, Jenny Nelson (2012).Chapter IE-2 - Organic Solar Cells. Practical Handbook of Photovoltaics (SecondEdition),volume(issue), pp-543-569

[4] Blom, P.W., Mihailetchi, V.D., Koster, L.J.A. and Markov, D.E., 2007. Device physics of polymer: fullerene bulk heterojunction solar cells. Advanced Materials, 19(12), pp.1551-1566.

[5] Karagiannidis, P.G., Kalfagiannis, N., Georgiou, D., Laskarakis, A., Hastas, N.A., Pitsalidis, C. and Logothetidis, S., 2012. Effects of buffer layer properties and annealing process on bulk heterojunction morphology and organic solar cell performance. Journal of Materials Chemistry, 22(29), pp.14624-14632.

[6] Scharber, M.C. and Sariciftci, N.S., 2013. Efficiency of bulk-heterojunction organic solar cells. Progress in polymer science, 38(12), pp.1929-1940.

[7] Zaidi, B. ed., 2018. Solar Panels and Photovoltaic Materials. BoDBooks on Demand.

[8] Giuseppe Pellicane, Mireille Megnidio-Tchoukouegno, Genene T. Mola, and Mesfin Tsige Surface enrichment driven by polymer topology, (2016), Phys. Rev. E 93, 050501.

[9] G. Workineh, Giuseppe Pellicane, and Mesfin Tsige, Tuning Solvent Quality Induces Morphological Phase Transitions in Miktoarm Star Polymer Films, Macromolecules, 2020, 53, 15, pp 61516162.

[10] Mamba, David S. Perry, Mesfin Tsige, and Giuseppe Pellicane, Toward the Rational Design of Organic Solar Photovoltaics: Application of Molecular Structure Methods to Donor Polymers, (2021). J. Phys. Chem. A, 125, 50, pp 1059310603.

[11] Dlamini, M.W. and Mola, G.T., 2019. Near-field enhanced performance of organic photovoltaic cells. Physica

B: Condensed Matter, 552, pp.78-83.
[12] Hamed, M.S.G. Oseni,S.O. Kumar,A. Sharma,G. Mola,G.T., 2020. Nickel sulphide nano-composite assisted hole transport in thin film polymer solar cells, Solar Energy, 195, pp.310-317
[13] Mola,G.T. Arbab,E.A.A. Taleatu, E.A. Kaviyarasu, K. Ahmad I. and M. Maaza, 2017. Growth and characterization of V2O5 thin film on conductive electrode, J. Microscopy, Vol. 265 (2), pp. 214-221
[14] Notarianni, M., Vernon, K., Chou, A., Aljada, M., Liu, J. and Motta, N., 2014. Plasmonic effect of gold nanoparticles in organic solar cells. Solar Energy, 106, pp.23-37.
[15] Kalfagiannis, N., Karagiannidis, P.G., Pitsalidis, C., Panagiotopoulos, N.T., Gravalidis, C., Kassavetis, S., Patsalas, P. and Logothetidis, S., 2012. Plasmonic silver nanoparticles for improved organic solar cells. Solar Energy Materials and Solar Cells, 104, pp.165-174.
[16] Mola, G.T., Mthethwa, M.C., Hamed, M.S., Adedeji, M.A., Mbuyise, X.G., Kumar, A., Sharma, G. and Zang, Y., 2020. Local surface plasmon resonance assisted energy harvesting in thin film organic solar cells. Journal of Alloys and Compounds, 856, p.158172.
[17] Petryayeva, E. and Krull, U.J., 2011. Localized surface plasmon resonance: Nanostructures, bioassays and biosensingA review. Analytica chimica acta, 706(1), pp.8-24.
[18] Lin, K.T., Lin, H. and Jia, B., 2020. Plasmonic nanostructures in photodetection, energy conversion and beyond. Nanophotonics, 9(10), pp.3135-3163.

[19] Boriskina, S.V., Ghasemi, H. and Chen, G., 2013. Plasmonic materials for energy: From physics to applications. Materials Today, 16(10), pp.375-386.
[20] Burgelman, M., Decock, K., Niemegeers, A., Verschraegen, J. and Degrave, S., 2016. SCAPS manual. February.
[21] Minbashi, M., Ghobadi, A., Ehsani, M.H., Dizaji, H.R. and Memarian, N., 2018. Simulation of high efficiency SnS-based solar cells with SCAPS. solar energy, 176, pp.520-525.
[22] KROON, R., LENES, M., HUMMELEN, J.C., BLOM, P.W. and DE BOER, B.E.R.T., 2008. Small Bandgap Polymers for Organic Solar Cells (Polymer Material Development in the Last 5 Years). Polymer Reviews, 48, pp.531-582.
[23] Oyedele, S.O. and Aka, B., 2017. Numerical simulation of varied buffer layer of solar cells based on cigs. Modeling and Numerical Simulation of Material Science, 7(03), p.33.

[24] Khelifi, S., Voroshazi, E., Spoltore, D., Piersimoni, F., Bertho, S., Aernouts, T., Manca, J., Lauwaert, J., Vrielinck, H. and Burgelman, M., 2014. Effect of light induced degradation on electrical transport and charge extraction in polythiophene: Fullerene (P3HT: PCBM) solar cells. Solar energy materials and solar cells, 120, pp.244-252.

[25] Omer, B.M., 2015. Effect of Valence Band Tail Width on the Open Circuit Voltage of P3HT: PCBM Bulk Heterojunction Solar Cell: AMPS-1D Simulation Study.
[26] Mandadapu, U., Vedanayakam, S.V. and Thyagarajan, K., 2017. Simulation and analysis of lead based perovskite solar cell using SCAPS-1D. Indian J. Sci. Technol, 10(11), pp.65-72.
[27] Nadeem, M.Y. and Ahmed, W., 2000. Optical properties of ZnS thin films. Turkish Journal of Physics, 24(5), pp.651-659.
[28] Huang, S.C., Lin, J.T., Haga, S., Chen, W.H. and Ho, K.Y., 2018, October. A Three-Terminal ZnS-based CIGS Solar Cell. In 2018 14th IEEE International Conference on Solid-State and Integrated Circuit Technology (ICSICT) (pp. 1-3). IEEE.
[29] Cao, J., Sun, T. and Grattan, K.T., 2014. Gold nanorod-based localized surface plasmon resonance biosensors: A review. Sensors and actuators B: Chemical, 195, pp.332-351.
[30] Jin, H., Olkkonen, J., Tuomikoski, M., Kopola, P., Maaninen, A. and Hast, J., 2010. Thickness dependence and solution-degradation effect in poly (3-hexylthiophene): phenyl-C61-butyric acid methyl ester based solar cells. Solar Energy Materials and Solar Cells, 94(3), pp.465-470.
[31] W. Dlamini, Mohammed S. G. Hamed, Xolani G. Mbuyise, Genene T. Mola, Improved energy harvesting using wellaligned ZnS nanoparticles in bulkheterojunction organic solar cell, (2020), Journal of Materials Science: Materials in Electronics, 31, pp 94159422
[32] Nam, Y.M., Huh, J. and Jo, W.H., 2010. Optimization of thickness and morphology of active layer for high performance of bulk-heterojunction organic solar cells. Solar Energy Materials and Solar Cells, 94(6), pp.1118-1124.
[33] Samanta, M., Chattopadhyay, K.K. and Bose, C., 2018, November. A Simulation Based Comparative Study of P3HT: PCBM and OC 1 C 10 PPV: PCBM Organic Solar Cells. In 2018 IEEE Electron Devices Kolkata Conference (EDKCON) (pp. 218-221). IEEE.
[34] Zekry, A., Shaker, A. and Salem, M., 2018. Solar cells and arrays: principles, analysis, and design. In Advances in renewable energies and power technologies (pp. 3-56). Elsevier.
[35] Kirchartz, T., Gong, W., Hawks, S.A., Agostinelli, T., MacKenzie, R.C., Yang, Y. and Nelson, J., 2012. Sensitivity of the MottSchottky analysis in organic solar cells. The Journal of Physical Chemistry C, 116(14), pp.7672-7680.
[36] Fabregat-Santiago, F., Garcia-Belmonte, G., Mora-Ser, I. and Bisquert, J., 2011. Characterization of nanostructured hybrid and organic solar cells by impedance spectroscopy. Physical chemistry chemical physics, 13(20), pp.9083-9118.
[37] Willis, S.M., Cheng, C., Assender, H.E. and Watt, A.A., 2011. Modified Mott-Schottky Analysis of Nanocrystal Solar Cells. arXiv preprint arXiv:1112.1623.
[38] Mehta, S.K., Kumar, S., Chaudhary, S., Bhasin, K.K. and Gradzielski, M., 2009. Evolution of ZnS nanoparticles via facile CTAB aqueous micellar solution route: a study on controlling parameters. Nanoscale research letters, 4, pp.17-28.
[39] Kuddus, A., Ismail, A.B.M. and Hossain, J., 2021. Design of a highly efficient CdTe-based dual-heterojunction solar cell with 44% predicted efficiency. Solar Energy, 221, pp.488-501.

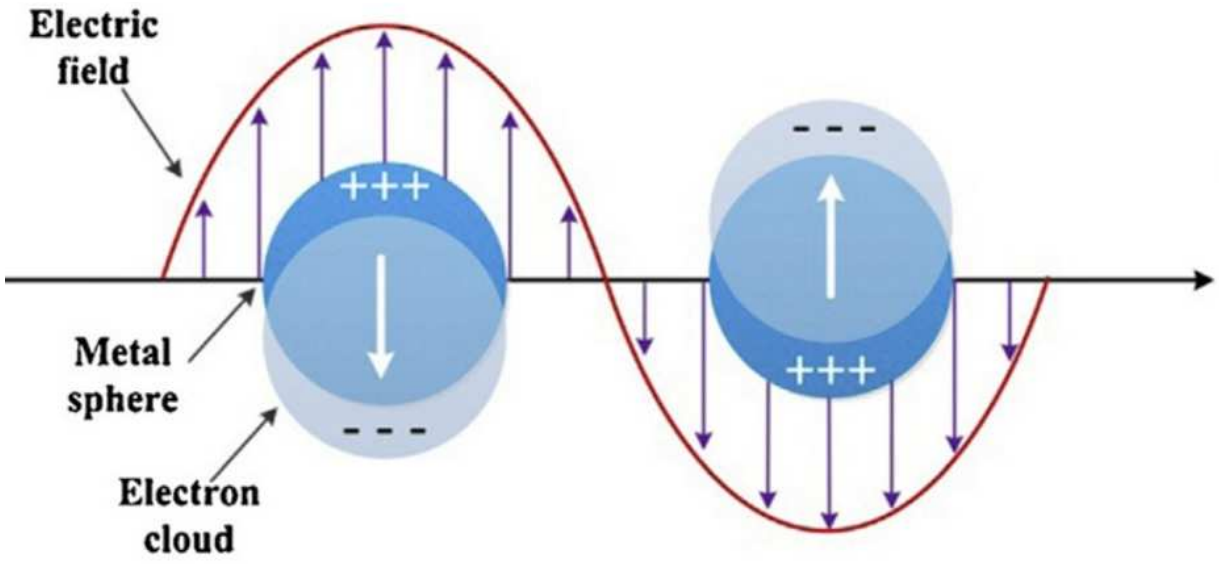

(a)

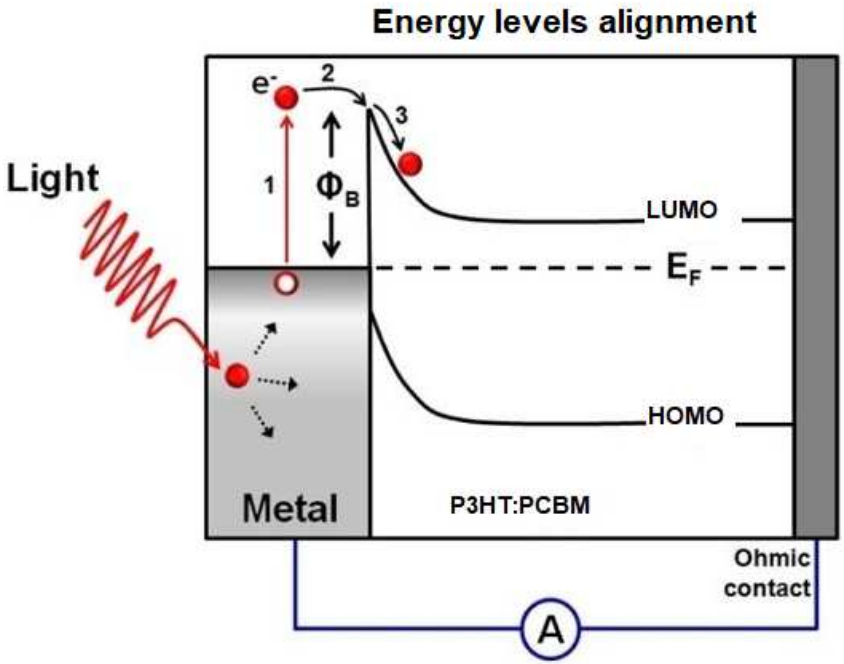

(b)

Figure

Click here to access/download;Figure;Fig_2.eps

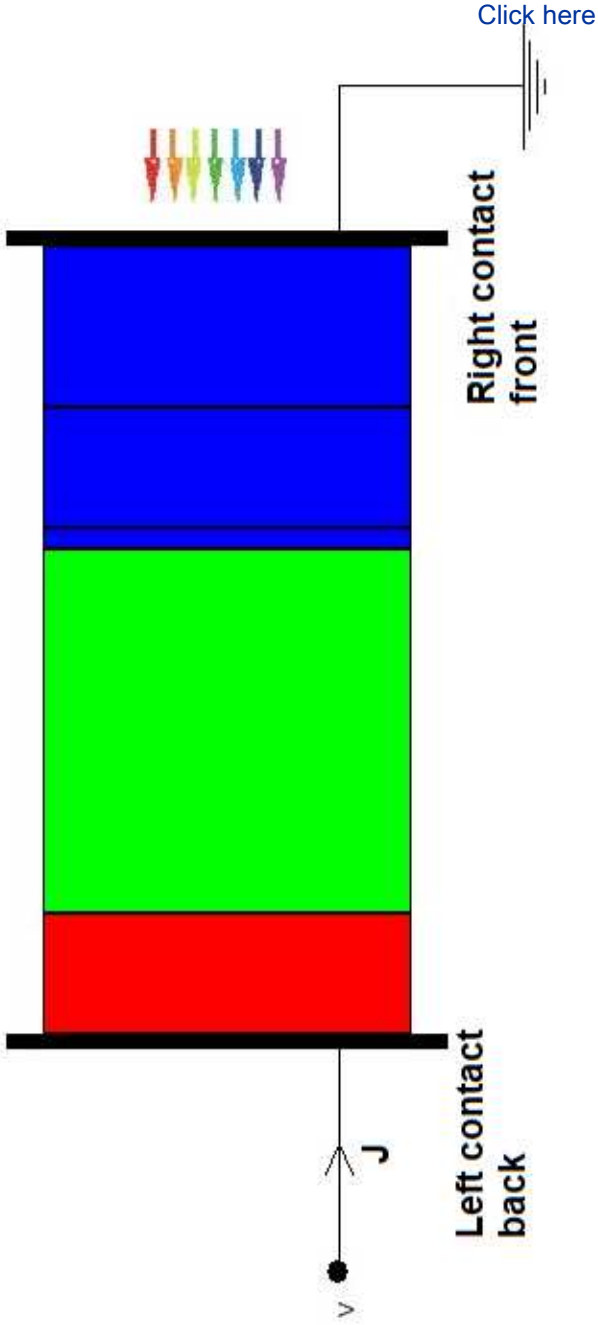

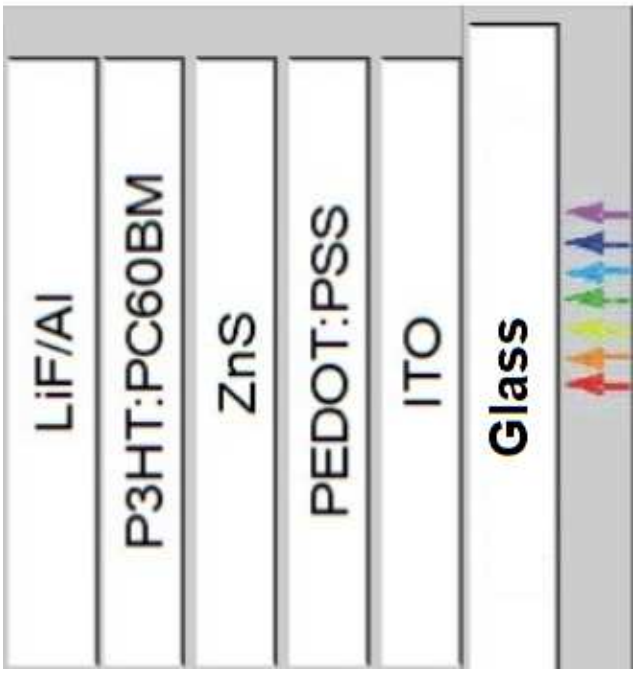

Figure

Click here to access/download;Figure;Fig_3.eps

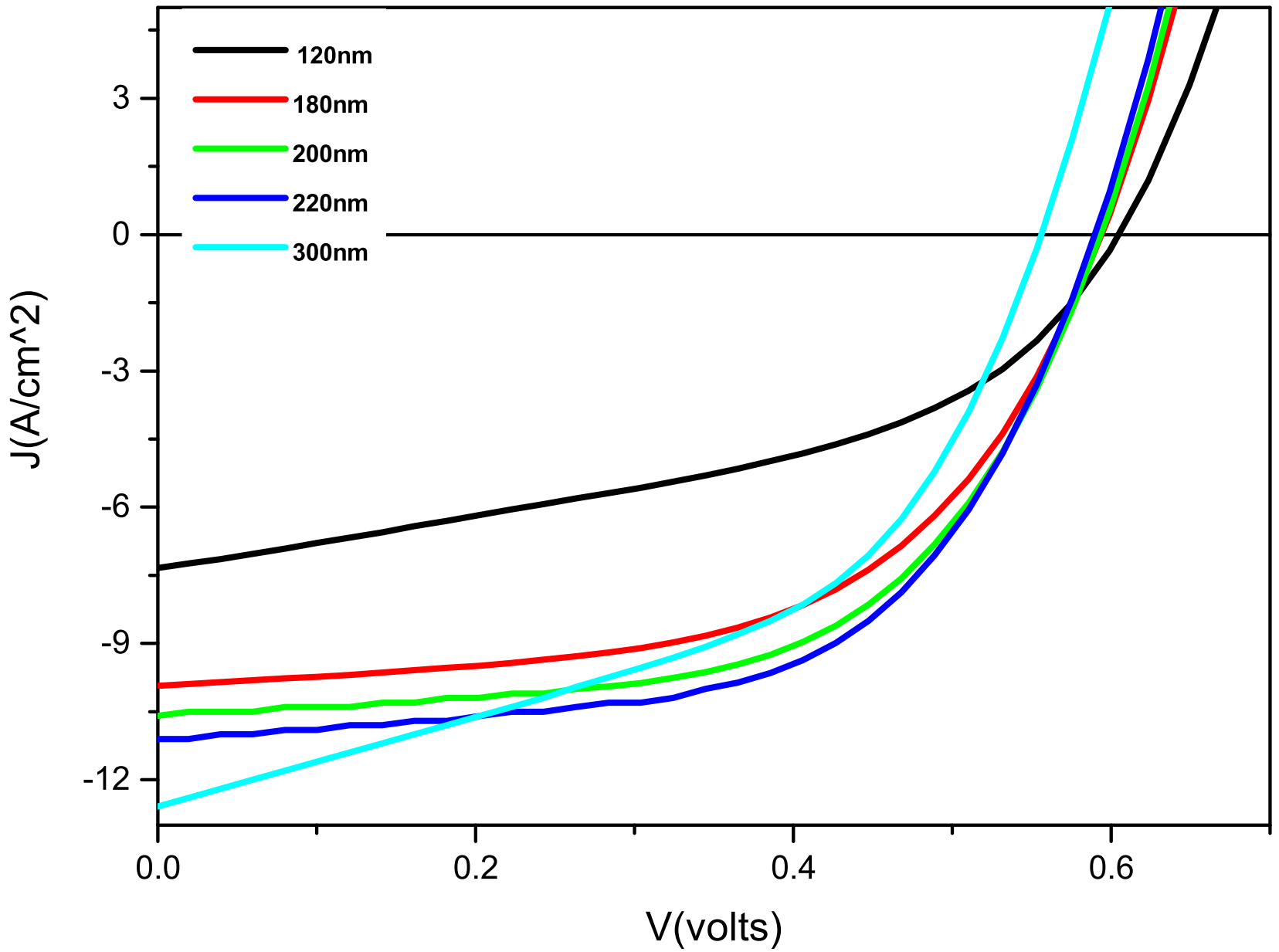

Figure

Click here to access/download;Figure;Fig_4.eps

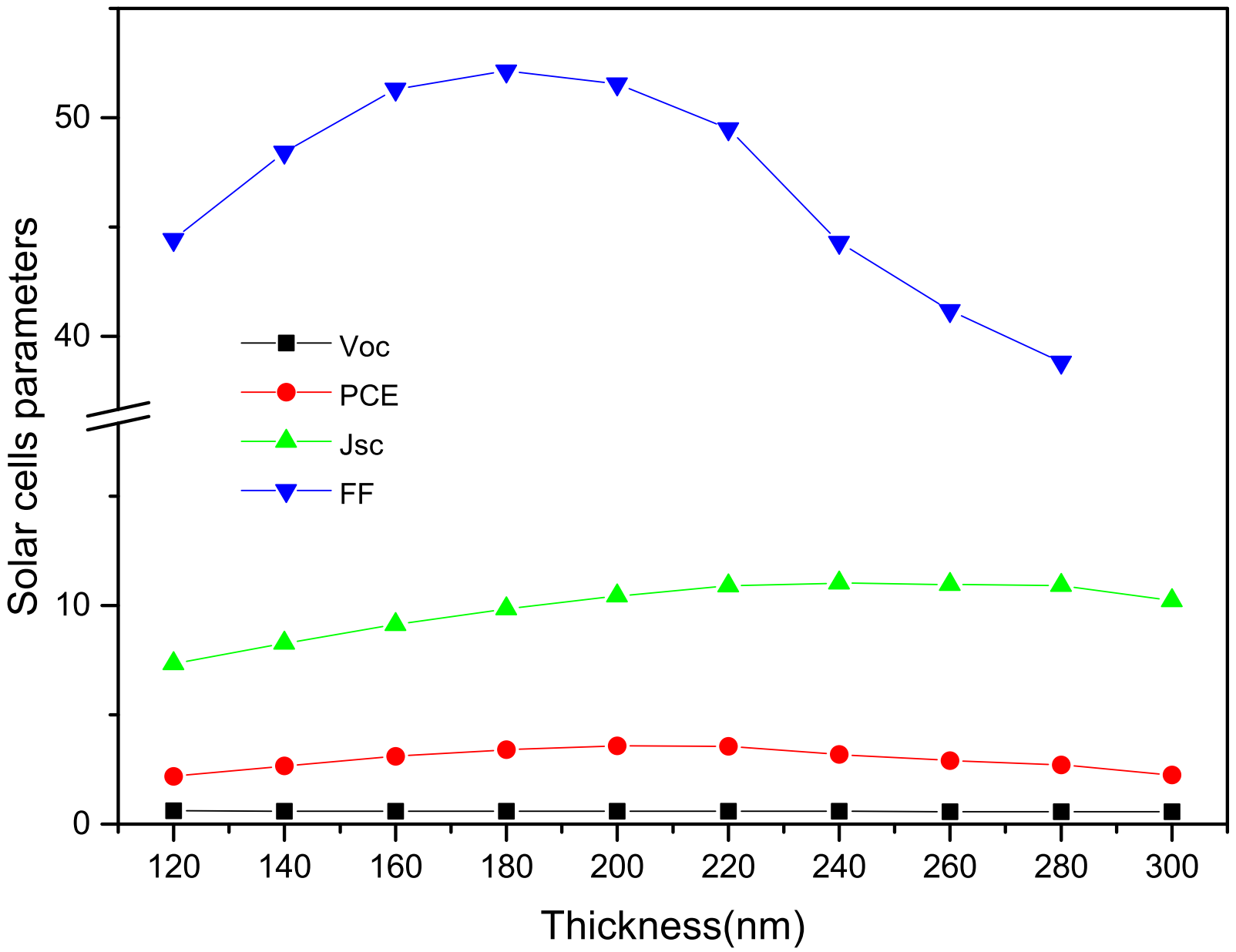

Figure

Click here to access/download;Figure;Fig_5.eps

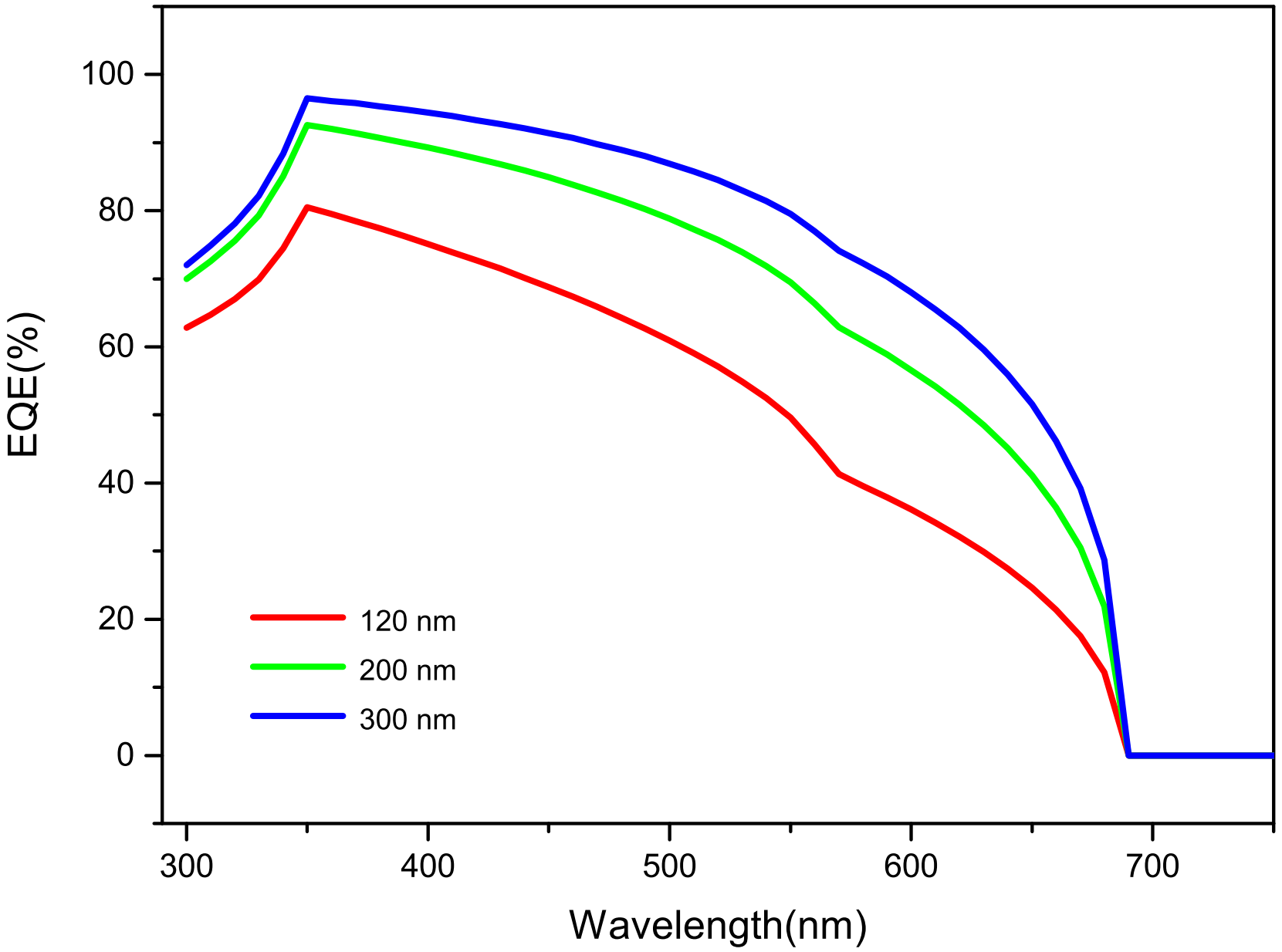

Figure

Click here to access/download;Figure;Fig_6.eps

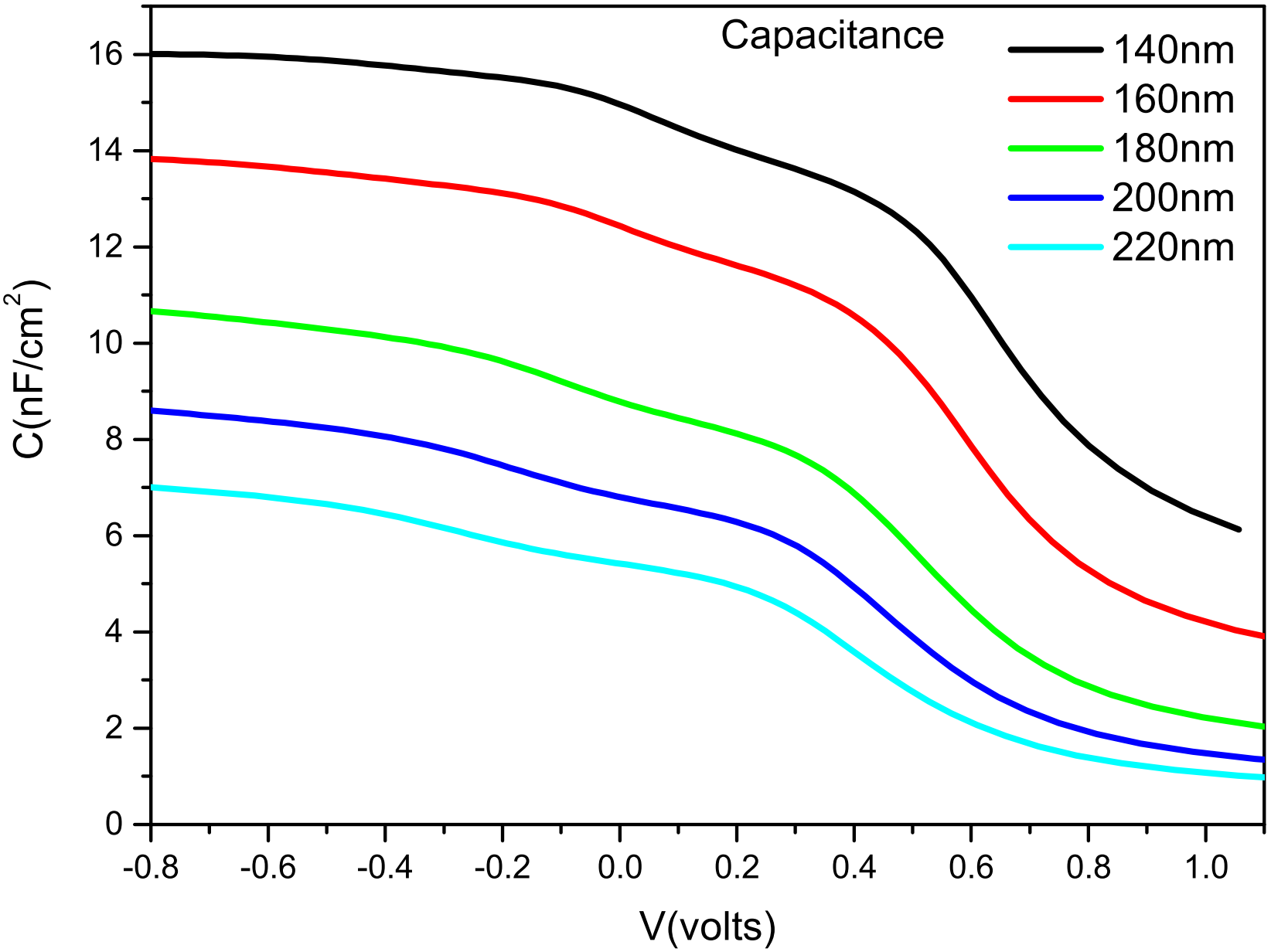

Figure

Click here to access/download;Figure;Fig_7.eps

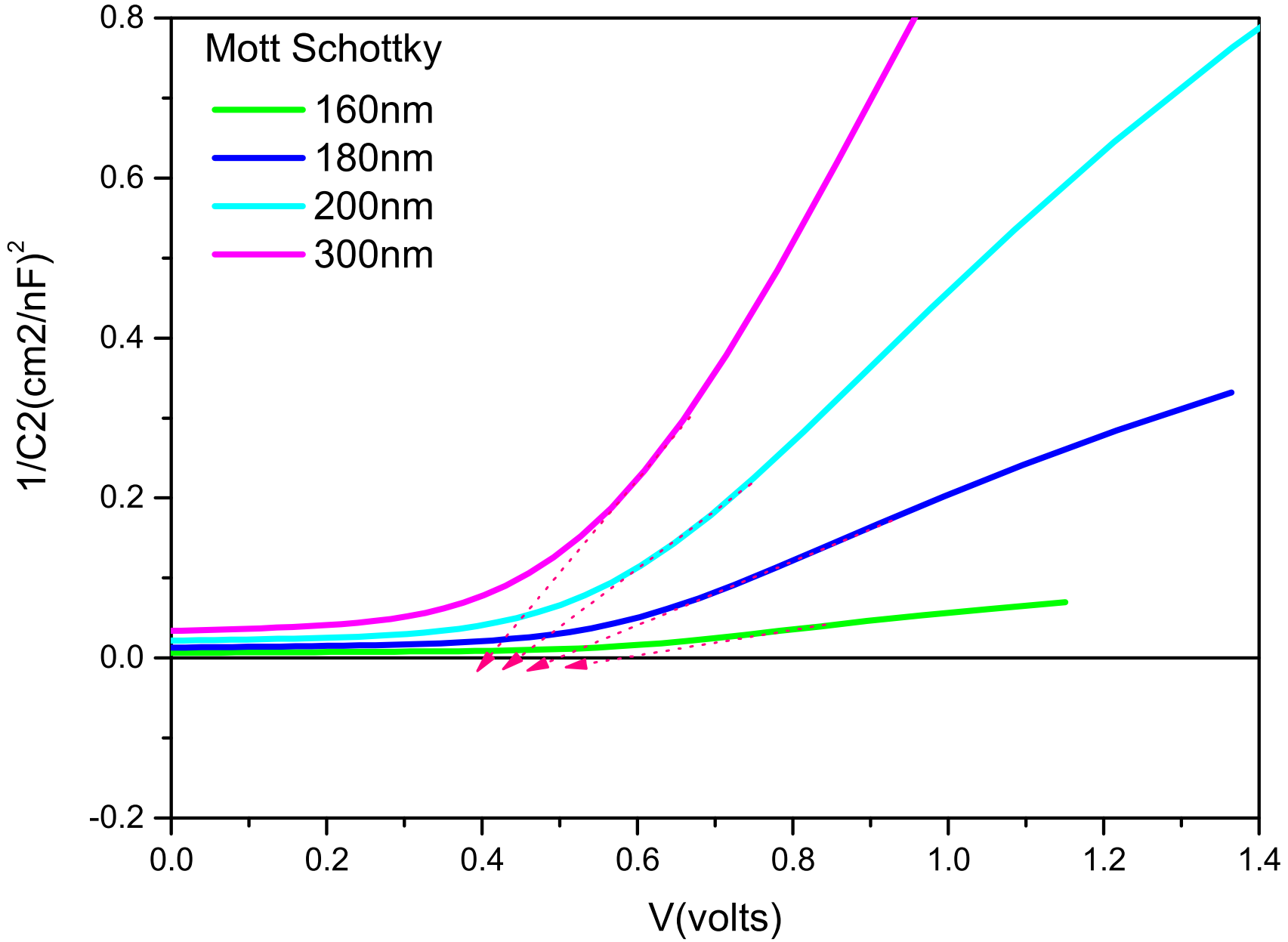

Figure

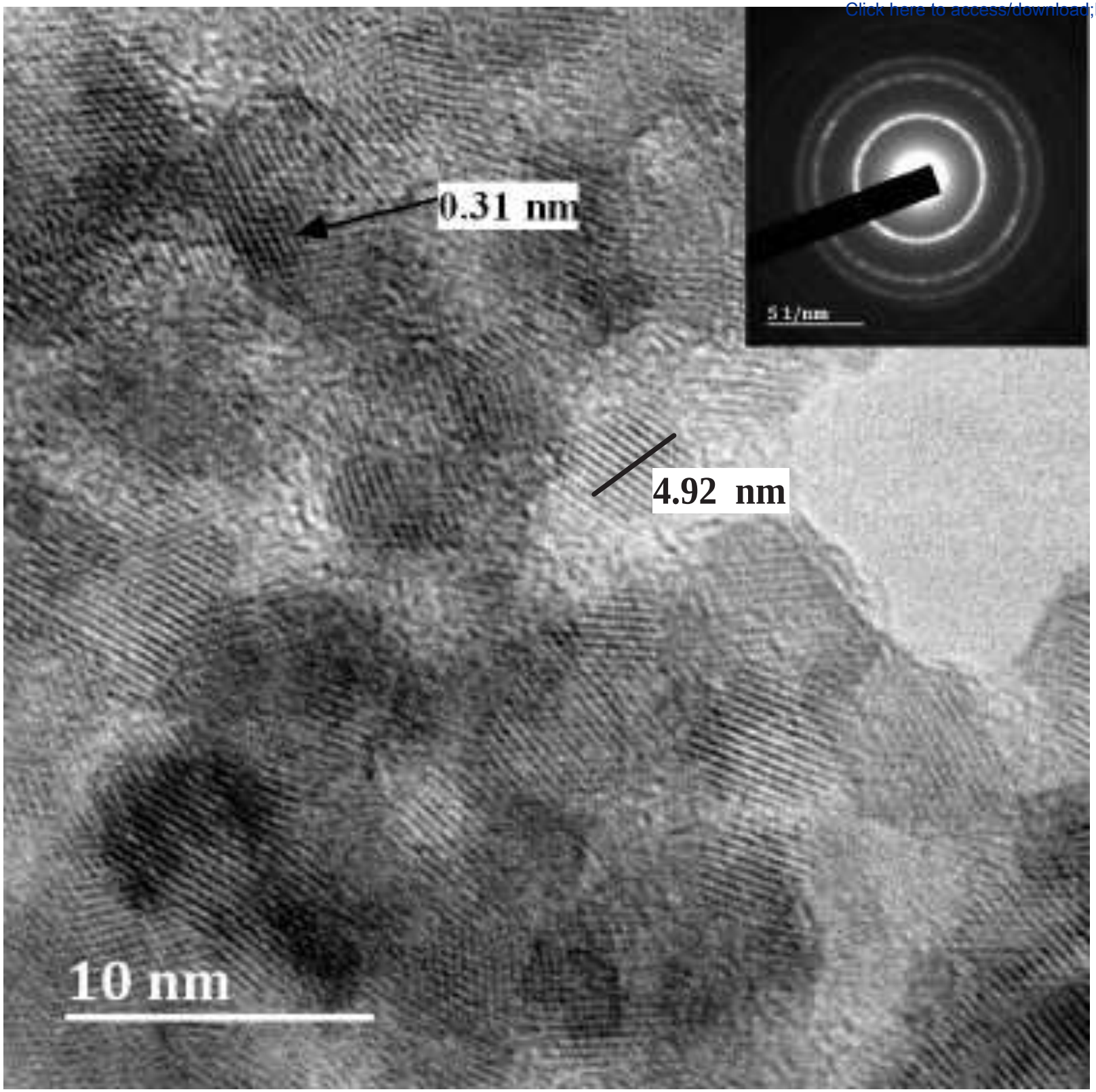

Figure

Click here to access/download;Figure;Fig_9.eps

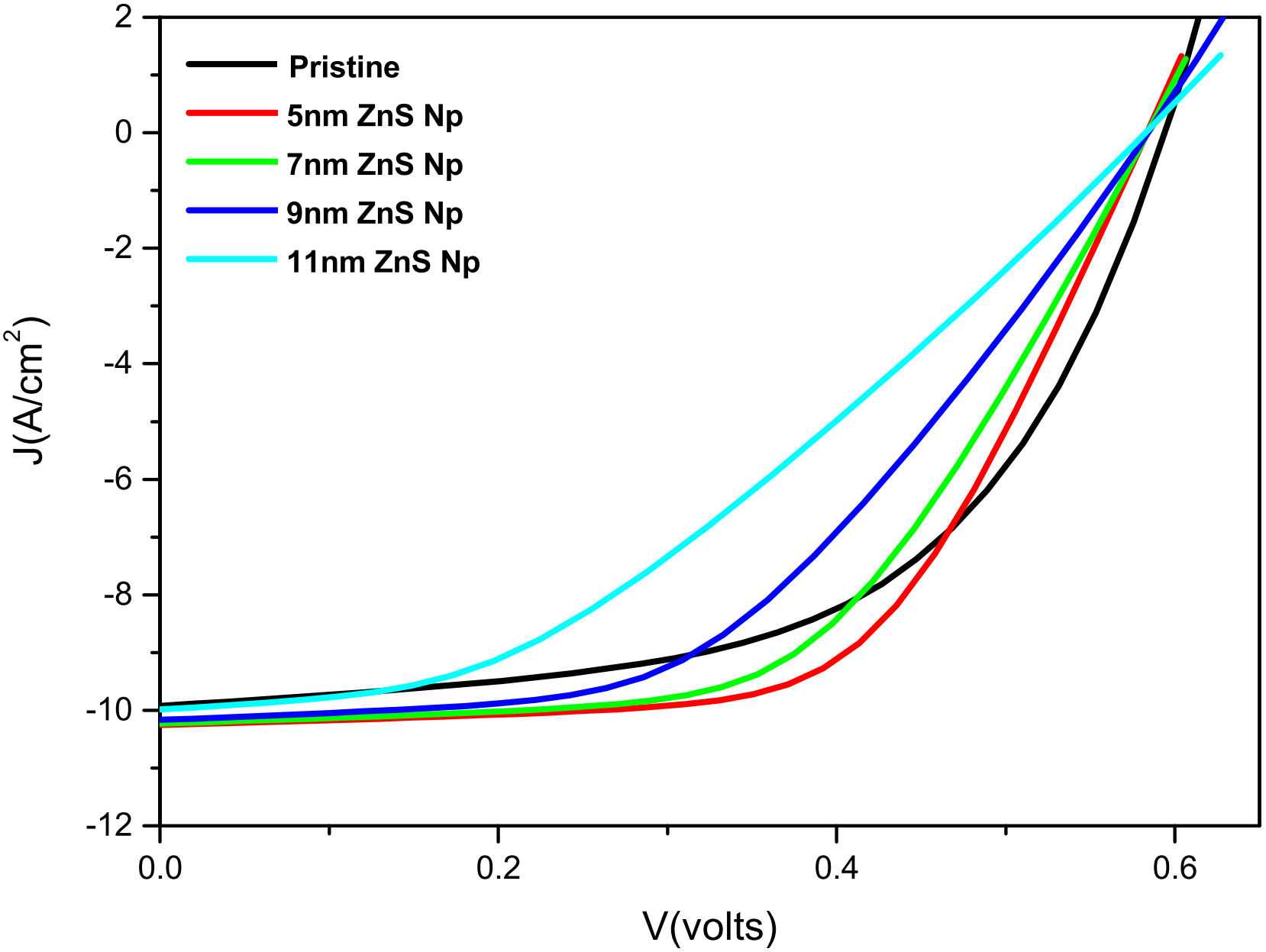

Figure

Click here to access/download;Figure;Fig_10.eps

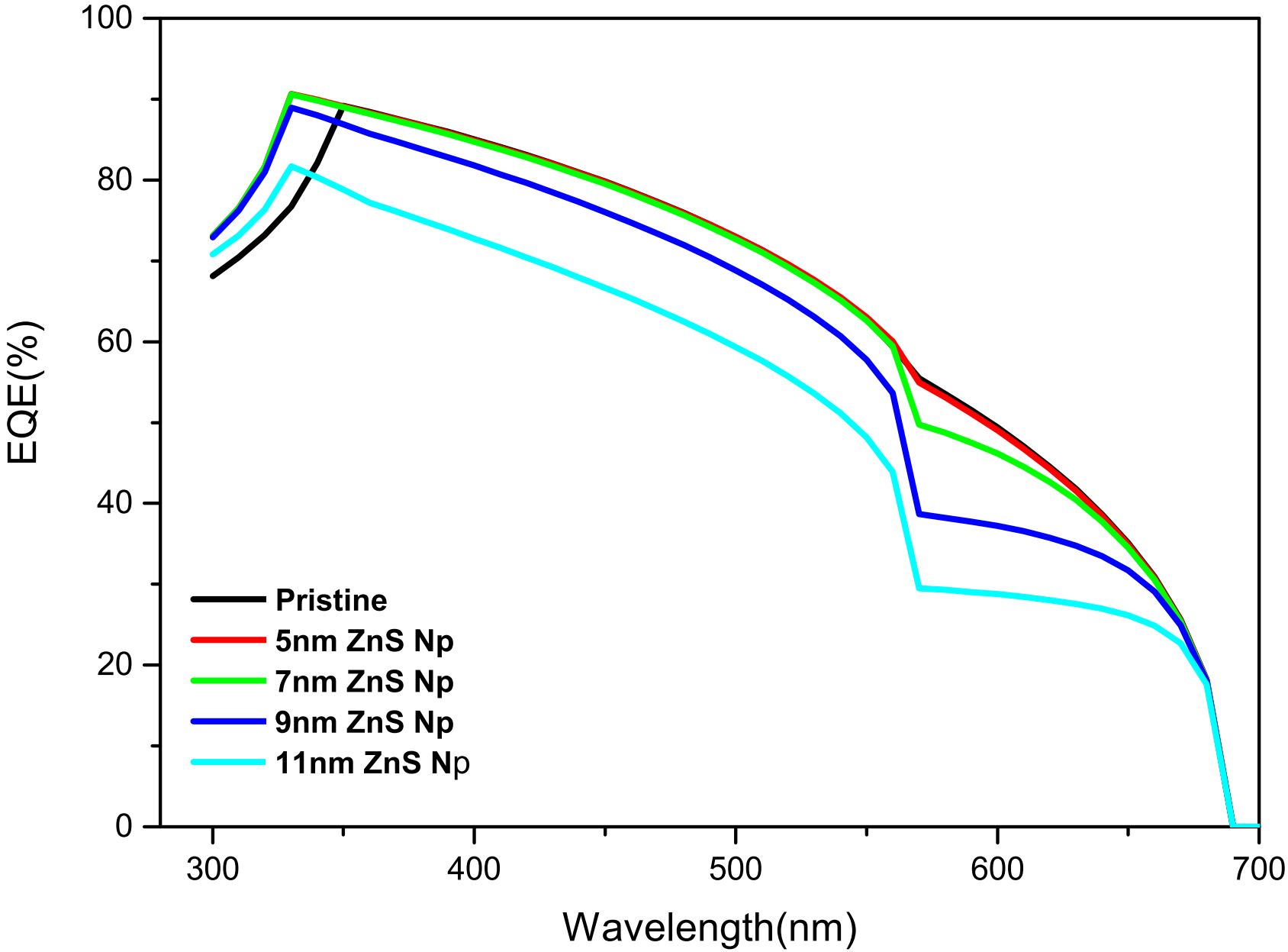

Highlights

- ZnS nano-particle is an effective mechanism to improve charge transport process in polymer solar cell.
- ZnS nano-particle can reduce charge recombination at the metal/polymer interfaces.
- The thickness of ZnS layer in the device architecture makes significant impact on the performance the solar cell

Declaration of interests

☒The authors declare that they have no known competing financial interests or personal relationships that could have appeared to influence the work reported in this paper.

☐The authors declare the following financial interests/personal relationships which may be considered as potential competing interests: